

Real-space simulation of 2D interacting quantum condensed matter systems

Francisco M. O. Brito

School of Physics, Engineering and Technology and York Centre for Quantum Technologies,
University of York, York YO10 5DD, United Kingdom

(Dated: May 8, 2024)

The proliferation of quantum fluctuations and long-range entanglement presents an outstanding challenge for the numerical simulation of quantum condensed matter systems with exotic ground states. In my thesis, I tackle two classes of two-dimensional interacting models on the honeycomb lattice: multi-orbital Hubbard models on zig zag terminated transition metal dichalcogenide nanoribbons (zTMDNRs) and generalised Kitaev models on a periodic hexagonal cluster.

In the first part of the thesis, I discuss novel results obtained in a comparative study of mean field theory (MFT) and determinant quantum Monte Carlo (DetQMC). Motivated by the difficulties posed by the fermion sign problem plaguing my DetQMC simulations, I carry out a survey of general purpose numerical methods.

The second part of the thesis addresses quantum spin liquids (QSLs) — which have attracted increasing attention — presenting a toolset of Chebyshev spectral methods developed during my PhD, namely: the finite temperature Chebyshev polynomial (FTCP) and the hybrid Lanczos-Chebyshev (HLC) methods. The first one enables studies of temperature dependence for quantities of experimental interest, such as the specific heat, with a two-fold speed-up with respect to state-of-the-art methods. The second one gives access to spectral functions efficiently and with unparalleled flexibility. I use it to obtain novel results for the spin susceptibility of the Kitaev-Ising model, unravelling dynamical signatures of a liquid-to-liquid transition.

OVERVIEW

Both classes of 2D interacting quantum models tackled in my thesis serve as minimal models for transition metal compounds with underlying honeycomb lattice structures and strong electron correlations. For the first class of models, electron-electron interactions are treated directly using MFT and DetQMC approaches. For the second, interactions are treated via effective quantum spin models, probed with methods based on Lanczos exact diagonalisation (ED), thermal pure quantum states (TPQ) and numerically exact expansions in Chebyshev polynomials

The first part of the thesis is devoted to the search for emerging magnetism at the one-dimensional edges of strongly correlated nanoribbons, where the reduced dimensionality gives rise to unique properties not present in the bulk. Here, I focus on transition metal dichalcogenides (TMDs), which are prominent members of the 2D materials family with numerous prospective technological applications. For instance, these semiconducting analogues of graphene are promising in the rapidly growing fields of opto-, spin-, and valleytronics.

The second part highlights the properties of phases with no magnetic order in a family of QSL candidate materials known as Kitaev magnets, among which are iridate compounds, such as Na_2IrO_3 . Rather than ordering magnetically, in these phases, fluctuating quantum spins remain disordered even at zero temperature, fractionalising into fermionic and gauge field degrees of freedom. This process leaves traces in the thermodynamics, for example in the specific heat and entropy, but also in the dynamics, in the form of distinct excitations, which can be probed experimentally, e.g. with inelastic neu-

tron scattering. In what follows, I summarise the work published in References [1, 2].

EDGE MAGNETISM IN TRANSITION METAL DICHALCOGENIDE NANORIBBONS

In the first part of the thesis, I model zTMDNRs using a generalised multi-orbital Hubbard model. The model is first approached using MFT, which points at a strong dependence of the ground state on the occupation of electronic states localised at the edges of the sample, or edge filling, ν_{edge} (see Fig. 1).

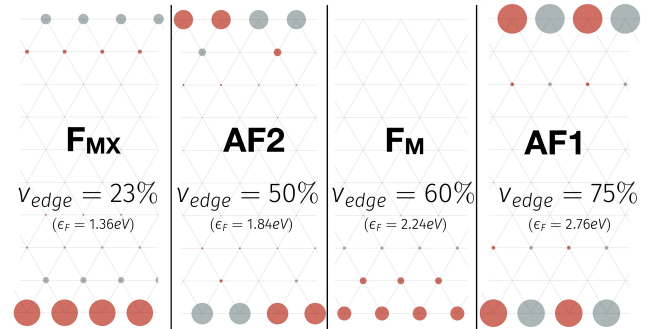


FIG. 1. Mean field magnetic ordering for fixed Hubbard interaction $U = 2.94$ eV at $T = 0$ for varying ν_{edge} . The size of the circles indicates the magnitude of the local spin density. Red corresponds to spin-up and grey to spin-down. Left to right: ferromagnetic phase on both edges (F_{MX}); edge-dimer (AF_2); ferromagnetic phase on the transition metal terminated edge (F_M); edge-antiferromagnetic phase (AF_1).

TMDs contain transition metals M = Mo, W and chalcogens X = S, Se, Te, in a 1:2 proportion. Thus, the edges of the ribbon are not equivalent and can be either transition metal or chalcogen terminated, respectively referred to as M- and X-edges. The unbiased, numerically exact DetQMC confirms the stability of one of the possible ground states —antiferromagnetic on both the M- and X-edges, with a paramagnetic bulk — albeit with quantitative differences, such as the critical Hubbard interaction for the onset of magnetic order (see Fig. 2).

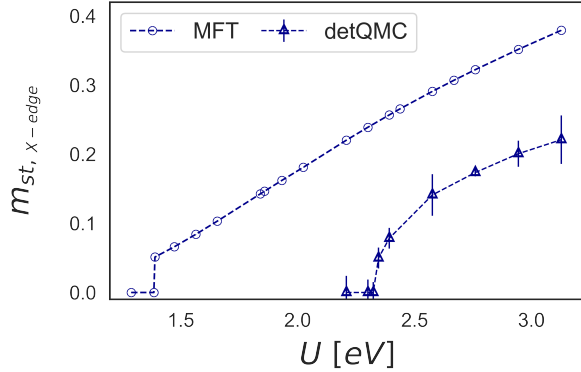


FIG. 2. Comparison between staggered magnetisations on the X-edge for AF1 obtained with MFT (circles) and DetQMC (triangles) as a function of the Hubbard interaction, U .

MFT is also found to overestimate long-range order, with DetQMC simulations confirming the onset of *quasi* long-range order instead, i.e. algebraic decay of spin-spin correlations along the edges of the ribbon (see Fig. 3).

The differences between the results of the two methods emphasise the importance of the unbiased nature of DetQMC. In this case, the latter allows one to gain deeper physical insight: despite the tendency for edge-antiferromagnetism in zig-zag terminated TMD nanoribbons at three-quarter edge filling, larger Hubbard interactions are required to achieve it and spin-spin correlations along the edges decay algebraically, rather than simply remaining constant, as predicted by MFT.

Unfortunately, DetQMC is severely plagued by the sign problem for this model. The variance of its estimators grows exponentially as most of the relevant edge fillings are reached and simulations are rendered unfeasibly expensive from the computational standpoint. Consequently, I am unable to confirm the wealth of phases predicted by MFT (shown in Fig. 1) using the unbiased DetQMC method.

REAL-SPACE SPECTRAL SIMULATION OF GENERALISED KITAEV MODELS

Motivated by the unbiased and numerically exact nature of the DetQMC approach, but also conscious of the

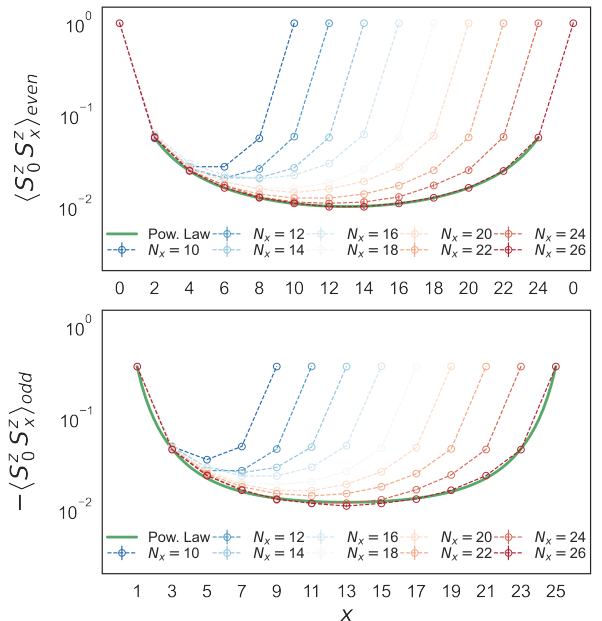


FIG. 3. Spin-spin correlations between even (top) and odd (bottom) sites along the X-edge for fixed Hubbard interaction. The green curves are fits to the DetQMC data using functions that decrease as a power law.

limitations imposed by the sign problem, in the second part of the thesis, I embark on a quest to develop a framework of numerical methods based on Chebyshev polynomial expansions. Despite remaining on the topic of 2D quantum many-body systems, I now focus on generalised Kitaev models hosting QSL phases. I apply a toolset of novel spectral methods developed during my PhD to compute both static (e.g. spin correlations) and dynamic (e.g. spin susceptibility) quantum observables in these paradigmatic frustrated systems with competing interactions that evade analytical approaches and are often sign problematic.

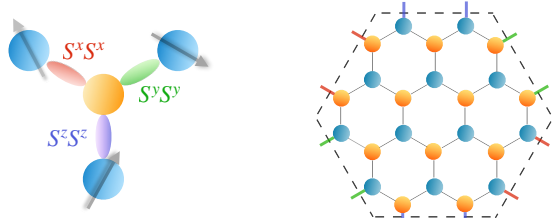


FIG. 4. (Left) Kitaev interaction. Nearest neighbour bonds coloured in red, green and purple (respectively $\gamma = x, y, z$ in the cartoon). The bond-directional character of the Kitaev interaction implies that to each bond corresponds a different type of interaction. Exchange frustration arises due to the nature of the interaction and it is not possible to find a spin configuration that simultaneously minimises the energy on all bonds. (Right) 24-spin hexagonal cluster with periodic boundary conditions.

The Kitaev model on the honeycomb lattice — obtained by considering bond-directional interactions (as outlined in the left panel of Fig. 4) — has attracted considerable interest because it is one of the rare examples of an exactly solvable microscopic model. Exchange frustration arises from the impossibility to simultaneously minimise the nearest neighbour interactions of Fig. 4, giving way to a fractionalised excitation spectrum of Majorana fermions coupled to a gauge field. Thus, Kitaev systems could serve as experimental probes for the fundamental physics of Majorana fermions and gauge fields.

For concreteness, I focus on the hexagonal cluster shown in the right panel of Fig. 4. I consider generalised Kitaev models, combining Kitaev interactions with Heisenberg (K-H) and Ising (K-I) interactions, which rule out exact solvability. I start by bench-marking my newly developed FTCP method for the pure Kitaev case. A comparison with other state-of-the-art methods indicates a 2-fold speed-up, among other advantageous convergence properties. My analysis is done as follows. I set out to obtain the nearest neighbour spin correlation, specific heat and entropy with ubiquitous methods, whilst carefully analysing convergence: I compute the minimum (i.e. optimal) number of iterations, such that the target functions are reliably captured within the desired accuracy at all temperatures. Naturally, the relevant convergence parameters need to be adjusted separately for each method due to their different characteristics. These are summarised in Table I. It is important to note that the results presented below not only agree with each other, but also with quantum Monte Carlo and exponential tensor renormalisation group studies, thus supporting the validity of my implementation for all methods.

TABLE I. Number of iterations (or Chebyshev polynomials) required for convergence for each method and CPU time per core per iteration. Notice that FTCP is twice as fast as TPQ.

Method	No. iterations	CPU time / core / it. [s]
TPQ	22000	0.57
FTLM	200	2.05
FTCP	7515	0.98

At first sight, Table I seems to indicate that FTLM is the most efficient method. However, notice that in Fig. 5, FTLM shows large low-temperature fluctuations, reaching about 26 times the fluctuations of FTCP (calculated from root-mean-square deviations). The inset of Fig. 5 shows that these fluctuations are larger for FTLM than for the other methods throughout the temperature range. Moreover, the total computational cost is dictated not only by the number of iterations, but also by the number of computationally costly operations per iteration (in this case, these are matrix-vector multiplications in an exponentially large vector space). This number is higher for FTLM than FTCP, leading to about twice the

average computer time per iteration (2.05 seconds with FTLM compared to 0.98 seconds with FTCP).

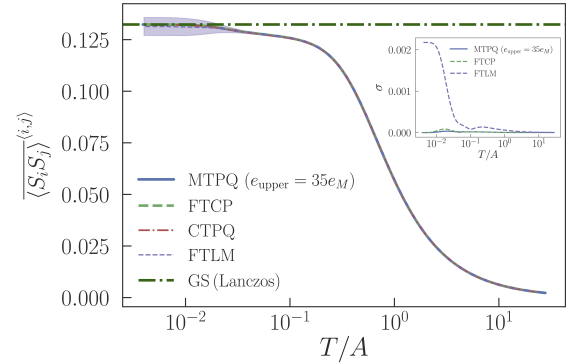


FIG. 5. Finite temperature nearest neighbour spin correlator computed with FTCP, FTLM and both microcanonical (M) and canonical (C) variants of TPQ for the Kitaev model on the 24-site hexagonal cluster. Under equal statistical circumstances, error bars are negligibly small, except for FTLM. For MTPQ, we use an energy upper bound of 35 times the maximum eigenvalue of the Hamiltonian obtained with Lanczos ED. Inset: Standard deviation of the nearest neighbour spin correlator. Despite having comparable (and thus not shown) fluctuations to MTPQ, CTPQ is numerically unstable at low temperature.

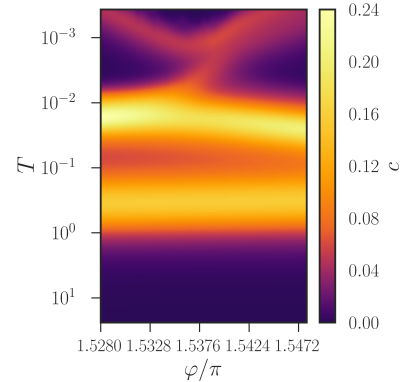


FIG. 6. Three-peak structure of the specific heat for the K-H model as the ratio between Heisenberg and Kitaev interactions (parametrised by φ — see Reference [2]) is increased.

Using FTCP, I have characterised thermal spin fractionalisation into Majorana fermions and a gauge field in the K-H model in terms of a multi-stage release of entropy of the relevant quasiparticles. This is accompanied by a multi-peak structure of the specific heat.

In Fig. 6, I show FTCP results for the specific heat of the K-H model on the hexagonal cluster. I find a three-peak structure of the specific heat that had not been described in the literature until this work. These results are consistent with thermal fractionalisation, suggesting a high temperature release of the entropy of the Majorana

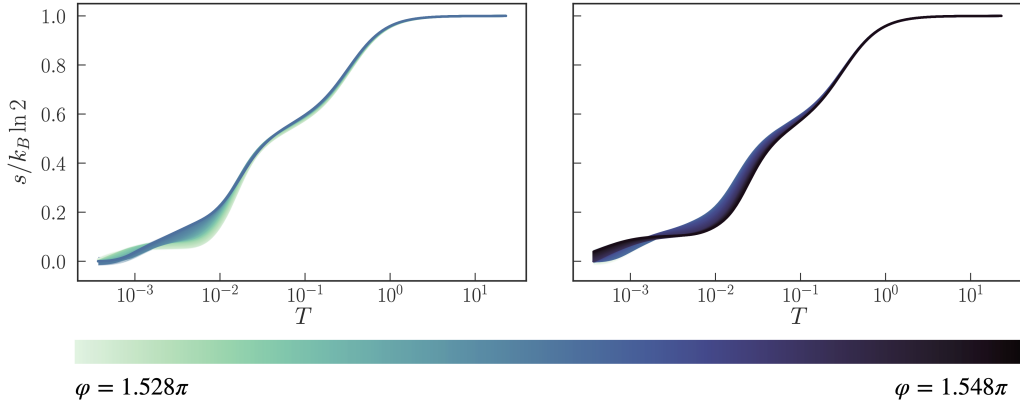


FIG. 7. Three-stage release of the entropy density in the K-H model. The colours correspond to a variation of the ratio between Heisenberg and Kitaev interaction, as indicated on the legend in the bottom. The results are separated in two panels to aid with visualisation.

fermions, followed by a low-temperature two-stage reconfiguration of the flux degrees of freedom inherited from the pure Kitaev model. The latter leads to the ground state configuration asymptotically for $T \lesssim 10^{-3}$, in units of the root of the sum of the squares of the coupling constants. As the pure Kitaev model is approached, the low-temperature peak diminishes, as it shifts towards lower temperature. In the Kitaev limit, the specific heat has a two-peak structure. Fig. 7 shows the three-stage release of entropy density corresponding to the three peaks of the specific heat. The results are also consistent with signs of spin fractionalisation at finite temperature, suggesting that near the Kitaev limit, the Heisenberg term might not completely modify the picture of Majorana fermions coupled to a gauge field. Instead, flux excitations could simply change in energy, with Fig. 7 pointing at the possibility of a frozen flux configuration for $T \in [10^{-3}, 10^{-2}]$. This is consistent with QSL candidate materials ordering at low temperature, but still showing signs of spin fractionalisation inherited from the Kitaev limit above the critical temperature for magnetic ordering.

Finally, I use the HLC method to study the dynamics of the K-I model, finding dynamical signatures of QSL and magnetically ordered phases. Here, I highlight novel results for the spin susceptibility. These have enabled the identification of clear signs of the quantum phase transitions in this model via a smooth change in the spin excitations at the quantum critical points. In particular, I analyse the liquid-to-liquid transition in the K-I model in terms of this change. The excitations of the Kitaev spin liquid phase in the K-I model are attributed to the introduction of a π -flux pair and subsequent reconfiguration of the Majorana fermions in this new background gauge field, which corresponds to a discrete peak structure in the spin susceptibility. Near zero frequency, the response vanishes due to the gapped nature of flux excitations. This characteristic peak structure of the Kitaev model fades away as a nematic liquid phase of the

K-I model is approached, and, in particular, the gap decreases and its distinctive low-frequency mode splits into a set of several low-frequency modes concentrated in a small range, precisely at the quantum critical point for the Kitaev QSL-nematic transition. The identification of dynamical signatures is relevant for the interpretation of experimental data that could potentially point at the existence of QSL phases in real compounds.

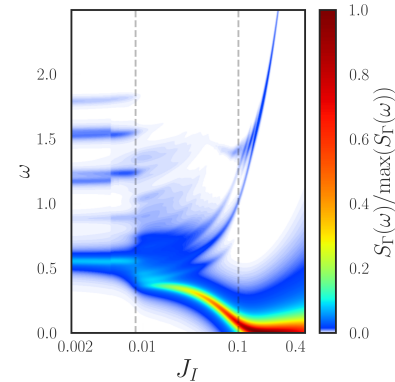


FIG. 8. Dynamical spin susceptibility, $S_\Gamma(\omega)$, of the K-I system for varying Ising interaction, J_I , normalised to its maximum value. The phase transitions are marked as grey dashed lines. The white space corresponds to a vanishing function as shown on the bottom of the colour bar.

In conclusion, this work highlights the power of unbiased methods, such as DetQMC and Chebyshev expansions, crucially with the latter being free from the sign problem, and thus giving access to a wider variety of quantum many-body systems.

-
- [1] F. M. O. Brito *et al.*, Phys. Rev. B **105**, 195130 (2022).
[2] F. M. O. Brito *et al.*, SciPost Phys. Core **7**, 006 (2024).